Enhanced Adsorption of a Protein-Nanocarrier Complex onto Cell Membranes through High Freeze Concentration by a Polyampholyte Cryoprotectant

Sana Ahmed,[†] Osato Miyawaki,[‡] and Kazuaki Matsumura[,†]*

[†]School of Materials Science, Japan Advanced Institute of Science and Technology, Nomi, Ishikawa 923-1292, Japan

[‡]Department of Food Science and Technology, Tokyo University of Marine Science and Technology, 4-5-7 Konan, Minato-ku, Tokyo, 108-8477, Japan

KEYWORDS: cytoplasmic delivery, freeze concentration factor, polyampholyte cryoprotectant, freezing point depression

ABSTRACT**:** Transportation of biomolecules into cells is of great importance in tissue engineering and as stimulation for antitumor immune cells. Previous freezing strategies at ultra-cold temperatures (−80 °C) used for intracellular transportation exhibit certain limitations such as extended time requirements and harsh delivery system conditions. Thus, the need remains to develop simplified methods for safe nanomaterial delivery. Here, we demonstrated a unique strategy based on ice crystallization-induced freeze concentration for protein intracellular delivery in combination with a polyampholyte cryoprotectant. We found that upon sustained lowering of temperatures from −6 to −20 °C over a short duration, the adsorption of proteins onto the peripheral cell membrane was markedly increased through facile ice crystallization-induced freeze concentration. Furthermore, we proposed a "freeze concentration factor" (α) that depends on the freezing point depression and is estimated from analysis of the fraction of frozen water. Notably, the α values of polyampholyte cryoprotectant were 6-fold higher than those of the currently used cryoprotectant dimethyl sulfoxide (DMSO) at particular temperatures of interest. Our results illustrate that the presence of a polyampholyte cryoprotectant significantly enhanced adsorption of the protein/nanocarrier complex onto membranes compared with that obtained with DMSO because of high freeze concentration. The present study demonstrated the direct relationship of freezing with penetration of proteins across the periphery of the cell membrane by means of increased concentration during freezing. These results may be useful in providing a guideline for the intracellular delivery of biomacromolecules using ice crystallization-induced continuous freezing combined with polyampholyte cryoprotectants.

INTRODUCTION

Bioactive molecules such as proteins play dynamic and diverse roles in biological systems; thus, their malfunction can lead to various diseases.[1] Intracellular protein delivery systems provide an

effective way to treat many diseases by facilitating the direct delivery of therapeutic proteins to cells.[2] Over the past several decades, researchers have focused on the establishment of new techniques for such delivery systems. Various reports have demonstrated the use of physical methods such as electroporation,[3] ultrasonication,[4] and microinjection[5] to facilitate the transport of proteins from the extracellular space to inside cells. However, if parameters such as voltage shock, current pulse, or ultrasound irradiation are applied to the cells for prolonged periods, some pores on the membrane exterior might enlarge or fail to close after membrane discharge, which causes cell damage or rupture. Methods utilizing physical forces such as electric fields or laser irradiation can thus create transient membrane holes or defects.[6] To reduce potential damage, numerous efforts have been made to promote active intracellular delivery of proteins, although success has been limited. To overcome these barriers, previously we developed a freeze concentration strategy for the effective cytoplasmic delivery of proteins.[7,8] The enhanced solute concentration afforded by the freezing approach was found to accumulate materials at the peripheral membrane and was highly beneficial for efficient protein internalization.

Freeze concentration is a physical process wherein at low temperature, water is transformed into ice crystals, which leads to the exclusion of solutes including protein-nanocarrier complexes. After exclusion, the concentration of solute complexes is relatively higher compared with the initial concentration.[9] Moreover, the use of freezing has been found to accelerate chemical reactions. For example, Kataoka et al. have demonstrated the use of a freezing process in click chemistry to facilitate condensation of the reactant.[10] In addition, Takenaka et al. found that the oxidation rate of nitrile by oxygen increased 10^5 times via a freeze concentration phenomenon.[11] In our previous work, we found that proteins from the protein-nanocarrier complexes were adsorbed from the complex onto the cell membrane and ultimately diffused inside the cells through the use of freezing,

specifically at −80 °C.[7, 8] However, proteins are known to be susceptible to aggregation and denaturation at below-freezing temperatures.[12,13] To prevent and protect against aggregation, the use of cryoprotectants for safe intracellular delivery is important in establishing an efficient cytoplasmic protein delivery system. Several cryoprotectants[14,15] such as ethylene glycol, glycerol, and dimethyl sulfoxide (DMSO) are commonly used to protect the protein structure. Furthermore, DMSO is often also utilized to improve the survival of cells during cryopreservation, although this chemical is itself cytotoxic. Accordingly, we developed a polyampholyte-based cryoprotectant that could substitute for the toxic commercial DMSO cryoprotectant in our previous studies.[16,17]

This increased concentration afforded by the freezing strategy for delivery of biomolecules was found to be very effective in earlier studies.[7,8] However, the use of ultra-cold temperatures (i.e., −80 °C) for prolonged duration render this system unfavorable for safe and convenient delivery. Additionally, quantification of the exact freeze concentration during freezing has not been investigated. However, Miyawaki et al. have proposed and generalized a new method for the estimation of the concentration factor during freezing by analyzing the freezable water and the fraction of frozen water.[18,19]

In this study, based on the generalized equation from Miyawaki[18] et al., we attempted to quantify concentration increases achieved through freezing at different temperatures in our system. This study also exemplified use of the modified freezing technology by means of simple ice-crystallization-induced continuous freezing to avoid extended process duration and use of extremely low temperatures in the delivery system **(Scheme 1).** Additionally, we also investigated the increased freeze concentration factor obtained by using the different cryoprotectants, DMSO and polyampholyte, in protein internalization through freezing. This fundamental study addresses

the direct relationship of freeze concentration based on ice crystallization with the internalization of biomolecules in a nanocarrier-based delivery system.

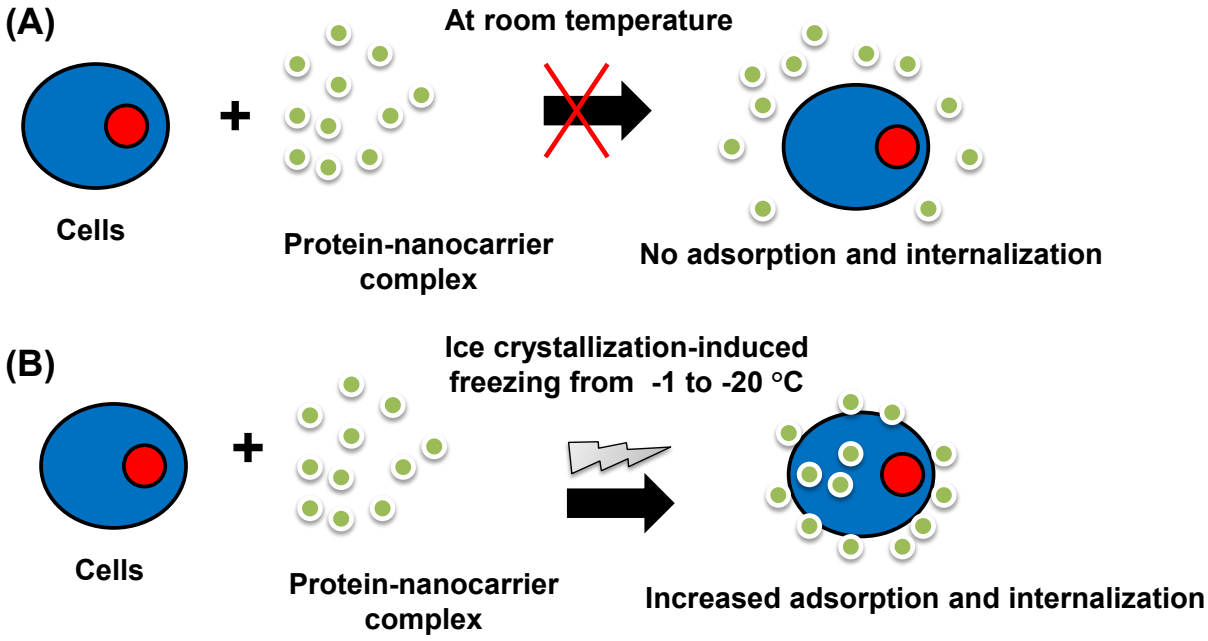

Scheme 1. Schematic illustration of the expected ice crystallization-induced freezing method for adsorption and internalization of protein nanocarrier complexes. (A) At room temperature, protein-nanocarrier complexes have difficulty in penetrating the cell membrane. (B) After applying stress through ice crystallization-induced freezing, the protein nanocarrier complexes are effectively adsorbed as well as internalized.

EXPERIMENTAL PROCEDURES

Preparation of Polyampholyte Cryoprotectant. A polyampholyte cryoprotectant was synthesized according to our previous report.[16,17] Briefly, a desirable ratio of succinic anhydride (SA, 1.3 g; Wako Pure Chem. Ind. Ltd. Osaka, Japan) to ε-poly-L-lysine (PLL) was mixed and reacted at 50 °C for 2 h to convert 65% of amino groups to carboxyl groups (**Scheme S1**). In the present study, polyampholyte cryoprotectant is represented as PLL-SA.

Preparation of Polyampholyte Nanoparticles. For the preparation of a carrier for protein delivery, a hydrophobic polyampholyte was synthesized based on our previous study.[7, 8] To obtain the polyampholyte nanoparticles, an aqueous solution of 25% (w/w) ε-PLL (10 mL, JNC Corp., Tokyo, Japan) and 3% molar ratio dodecenylsuccinic anhydride (DDSA; Wako Pure Chem. Ind. Ltd, Osaka, Japan) was heated at 100 °C and allowed to react for 2 h to obtain hydrophobically modified PLL (**Scheme 2**). Next, SA was added at 10% molar ratio ($COOH/NH_2$) and allowed to react at 50 °C for 2 h. The degree of substitution of SA and DDSA was obtained by 1H-nuclear magnetic resonance (^{1}H-NMR). The spectra were acquired on a Bruker AVANCE III 400 spectrometer (Bruker Biospin Inc., Fällanden, Switzerland) in D_2O at 25 °C. Here, we denoted hydrophobic polyampholytes for this study as PLL-DDSA (3)-SA(10), indicating that 3% molar ratio of the amino group was converted to DDSA and a 10% molar ratio of the amino groups from PLL had been substituted with SA.

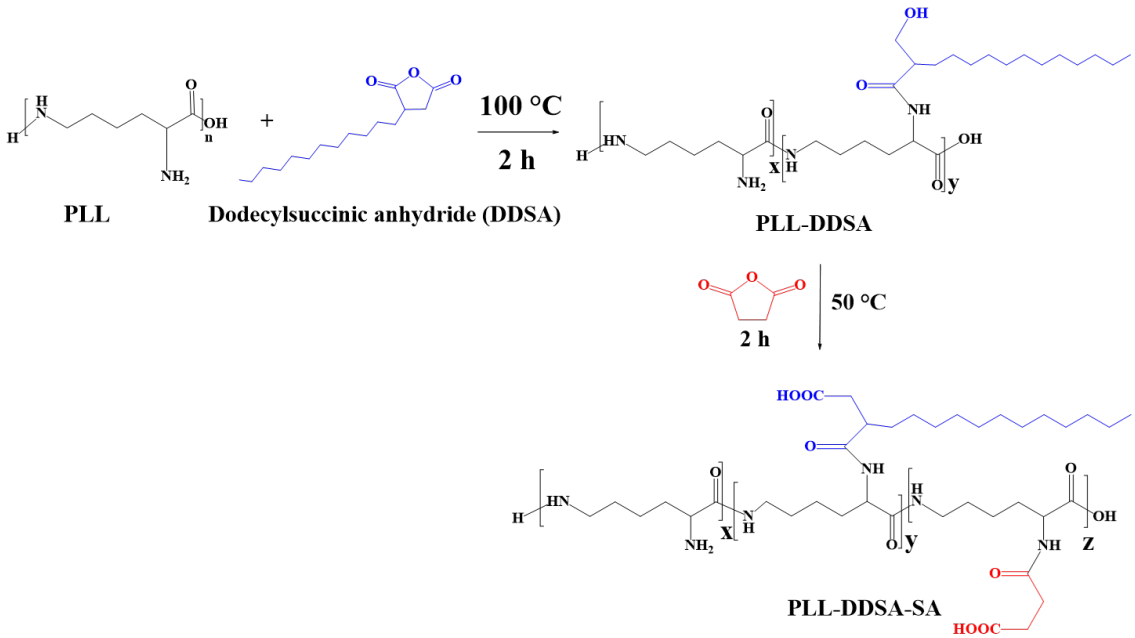

y= 3%; z= 10% ; x= 87%

Scheme 2. Synthetic scheme for the preparation of hydrophobic polyampholytes (PLL-DDSA-SA).

Preparation of Protein and Polyampholyte Nanoparticle Complexes (OVA-Loaded PLL-DDSA (3)-SA(10)). To prepare proteins and the polyampholyte nanoparticle complex, ovalbumin (OVA) was selected as a model protein. Polyampholyte nanoparticles (10 mg/mL) were mixed with OVA protein (2 mg/mL) with a final volume of 0.5 mL in phosphate-buffered saline without calcium and magnesium ions (PBS(−)) and incubated for 2 h at room temperature. The mixture was then centrifuged for 4 min at 11,200 *g* using a centrifugal filter (cut off: 100 kDa) to separate the unabsorbed and adsorbed proteins.

Size and Zeta Potential Measurements. The average hydrodynamic diameter of polyampholytes was measured by dynamic light scattering and the zeta potential calculated using Zetasizer 3000 (Malvern Instruments, Worcestershire, UK) with a scattering angle of 135°. Data were obtained as the average of three measurements carried out on different samples.

Determination of Freezing Point of Cryoprotectants such as DMSO, Polyampholytes, and Protein-Loaded Polyampholyte Nanoparticles. To investigate the freeze concentration factor in our system, we determined the freezing point as determined in a previous study.[18] Briefly, the samples (3 mL) were put into plastic tubes (15 mm in diameter) along with a thermistor (0.01 °C in accuracy: D641, TaKaRa Thermistor, Yokohama, Japan), and frozen completely at −20 °C in a cooling bath (NCB-3200, Eyela, Tokyo, Japan). Next, the samples were warmed by stirring with a vortex mixer to melt at room temperature. The change in the temperature was recorded using a PRR-5021 recording instrument (Toa DKK, Tokyo, Japan). The freezing point was investigated using melting curve analysis.[18]

Fluorescence Labeling of Polyampholyte Nanoparticles and Proteins. OVA (10 mg) and fluorescein isothiocyanate (FITC, Dojindo, Kumamoto, Japan) (1 mg/mL) were dissolved in sodium bicarbonate buffer solution (1 mL; 0.5 M, pH 9.0) with gentle stirring and incubated at 4 °C overnight with subsequent dialysis (molecular weight cut off: 3 kDa, Spectra/Por, Spectrum Laboratories, Inc., Rancho Dominguez, CA, USA) for three days against water, and finally freeze-dried.[20] To visualize both OVA and polyampholytes during the same observation, we labeled OVA protein with a different dye, i.e., Texas red sulfonyl chloride (TR) solution. For protein labeling with TR, OVA (2 mg) was dissolved in chilled buffer (sodium bicarbonate, 0.1 M) to which 50 μL TR solution (Dojindo, 1 mg in 50 μL of acetonitrile) was added and mixed rapidly. Then, the reaction was desalted using a desalting column (30 K) that was equilibrated using PBS(–) buffer. Polyampholyte nanoparticles were labeled with fluorescent FITC dye. For labeling, a solution of 25% (w/w) aqueous PLL was reacted with FITC at a 1/10,000 molar ratio for 24 h at room temperature. The resultant solution was purified by dialysis (molecular weight cutoff 3 kDa) against water for 3 days.[7, 8] After labeling, the same procedure was used for the preparation of hydrophobically modified polyampholytes.

Cell Culture. NIH3T3 fibroblast cells (American Type Culture Collection, Manassas, VA, USA) were cultured in Dulbecco's modified Eagle's medium (DMEM; Sigma-Aldrich, St. Louis, MO, USA) supplemented with 10% calf serum (CS) at 37 °C under 5% CO_2 in a humidified atmosphere. When the cells reached 80% confluence, they were removed using 0.25% (w/v) trypsin containing 0.02% (w/v) ethylenediamine tetraacetic acid in PBS(−) and seeded on a new tissue culture plate for subculture.

Cytotoxicity of Polyampholytes. Cytotoxicity was determined by 3-(4,5-dimethyl thial-2yl)-2,5-diphenyltetrazalium bromide (MTT) assay.[7, 8] NIH3T3 cells at a density of 1×10^3 cells/mL

were cultured in each well and incubated under saturated humidity conditions at 37 °C in the presence of 5% CO_2. After 72 h of incubation at 37 °C, 0.1 mL of media at different concentrations of polyampholyte was added to the cells and incubated for 24 h. Then, MTT solution (0.1 mL, 300 μg/mL in medium) was added to the cells. The cells were incubated for 4 h at 37 °C. After incubation, the solutions were removed and replaced by DMSO (100 μL) and allowed to stand for 15 min to allow a complete reaction. The resulting color intensity was measured using a microplate reader (VersaMax, Molecular Devices Co., Sunnyvale, CA, USA) at 540 nm, and was proportional to the number of viable cells. The toxicity was measured as the concentration of the compound that caused a 50% reduction in MTT uptake by a treated cell culture compared with the untreated control culture (IC_{50}).

Freezing and Thawing Conditions of Cell-Loaded Protein-Nanocarrier Complexes. FITC-labeled OVA protein-loaded polyampholyte nanoparticles (2 mg protein and 1 w/w% nanoparticles in the cell suspension) were prepared in the presence of cryoprotective solution (10% DMSO or 10% PLL-SA) in DMEM without fetal bovine serum and sterilized using a 0.22-μm syringe filter. NIH3T3 cells at a density of 1×10^4 cells/mL containing protein-loaded polyampholyte nanoparticles (500 μL) were transferred into a cryo-straw using a freeze controller cryobath (Cryologic, Victoria, Australia). The samples were cooled at the rate of 1 °C/min. At particular temperatures (−6, −9, −12, −15, −18, and −20 °C), the temperature was held and the ice seeding was performed for approximately 1 min to all samples for inducing ice crystallization. The ice seeding was performed manually using cold tweezers (pre-chilled with liquid nitrogen) at each temperature. After 10 min of incubation to complete the freezing, the straw solutions at each temperature were withdrawn and thawed by immersion in water at 37 °C. The thawed solutions were then diluted 10-fold with medium and solutions were centrifuged at 112 *g* for 4 min. The

solution was then replaced with fresh DMEM. The cell viability was calculated using a trypan blue assay as the number of viable cells divided by the total cells. The adsorption of OVA protein-loaded polyampholyte nanoparticles was observed using confocal laser scanning microscopy (CLSM, FV-1000-D; Olympus, Tokyo, Japan).

In Situ Fluorescence Microscopic Observation of Cell-Loaded Protein-Nanocarrier Complexes during Freezing. TR-OVA-loaded FITC-polyampholyte complexes (10 μL) in the presence of 10% polyampholyte cryoprotectant were placed on a slide, covered, and loaded on a cooling stage (Linkam 10002L Cooling Stage, Japan High Tech., Fukuoka, Japan) using a programmable freezing rate of 1 °C/min. The same freezing protocol was utilized as described above, except instead of thawing, the cells were directly observed during freezing through a microscope. The images were directly captured with a fluorescence microscope using the Keyence Biozero 800 system (Osaka, Japan).

Internalization of Protein-Polyampholyte Nanocarrier Complexes. After treatment at different temperatures as described above, the NIH3T3 cells were thawed at 37 °C and washed three times using cell culture medium with 10% of CS. The cells were then seeded onto 35-mm glass bottom dishes and medium (1 mL) was added. After incubation for 48 h, the attached cells were washed with PBS and internalization of protein-nanocarrier complexes was observed using CLSM.

Statistical Analysis All data are expressed as the mean ± standard deviation (SD). All experiments were conducted in triplicate. Statistical comparison of groups was performed using a 2-tailed ANOVA with Scheffe post-hoc correction. Differences were considered statistically significant at $P<0.05$.

RESULTS

Preparation of Polyampholyte Cryoprotectant. The polyampholyte cryoprotectant was synthesized by using ε-PLL, an L-lysine homopolymer biosynthesized by *Streptomyces* species. Cryoprotectant was prepared by changing the appropriate ratio of amino groups present in ε-PLL into carboxyl groups by succinylation with succinic anhydride (65 mol%) as described in our previous study (**Scheme S1**).[17,18] This potent polyampholyte cryoprotectant in 10% aqueous solution has been reported to exhibit high cryopreservation of various cell lines with low toxicity. The success of modification into PLL was verified using ^{1}H NMR (**Figure S1A**) analysis using equation 1:

$$\text{Degree of substitution for SA (\%)} = (2*A_{\delta 2.4}/4*A_{\delta 1.5\text{-}1.8})*100 \quad (1)$$

where $A_{\delta 1.5\text{-}1.8}$ is the integral of intact methylene protons of PLL located at 1.5–1.8 ppm and $A_{\delta 2.4}$ is the integral of the methylene peak of SA. We found that SA was modified onto PLL at 61.2% according to this equation.

Synthesis of Hydrophobic Polyampholytes for the Preparation of Nanocarriers. An important advance in nanomedicine was the development of nanocarriers that are able to respond to physical and chemical stimuli to enhance the efficacy of therapeutics and promote delivery at the target site.[21] Nanocarriers such as micelles,[22] liposomes,[23] or nanoparticles[24] are often utilized for the delivery of therapeutic molecules to disease site to exert clinical benefit. However, many have exhibited limitations such as cytotoxicity, low stability, and low efficacy.[25,26] To address this problem, we developed a polyampholyte-based nanocarrier through modification by DDSA using ε-PLL in our previous research.[7] The successful modification of DDSA and SA was verified by ^{1}H NMR analysis as shown in **Figure S1B**. The degree of substitution of DDSA and SA was found to be 2.7 % and 10.48 %, respectively, as determined by ^{1}H NMR according to equations 2 and 3:

Degree of substitution for DDSA (%) = $(2*A_{\delta 0.74}/3*A_{\delta 1.5\text{-}1.8})*100$ (2)

Degree of substitution for SA (%) = $(2*A_{\delta 2.4}/4*A_{\delta 1.5\text{-}1.8})*100$ (3)

where $A_{\delta 0.74}$ is the integral peak of the methyl group of DDSA located at 0.74 ppm and $A_{\delta 2.4}$ is the integral of the methylene peak of SA located at 2.4 ppm. Moreover, the integral peak of methylene groups in intact PLL was in the range of 1.5 to 1.8 ppm. Next, we investigated the effect of surface charge and particle size of polyampholytes after modification with SA and DDSA.

Particle Size and Zeta Potential of Polyampholyte Nanoparticles. Hydrophobic polyampholyte nanoparticle size and surface potential in aqueous media were determined. As shown in **Figure S2A**, the hydrophobic polyampholytes PLL-DDSA (3)-SA (10) were approximately 16.68 ± 0.35 nm in diameter with a polydispersity index of 0.35, indicating nanoparticle uniformity (**Figure S2A**). This result was complementary to our previous results.[7] Moreover, the surface potential of PLL-DDSA (3)-SA(10) was reduced compared with that of intact PLL. This result further confirms the successful modification of DDSA and SA into PLL (**Figure S2B**).

Preparation and Characterization of the Protein-Nanocarrier Complex. For the delivery of proteins, we chose OVA, a 45 kDa globular protein that is commonly used in many studies as a model vaccine antigen.[27–29] For the formulation of protein nanocarrier complexes, the OVA proteins can be easily bound with polyampholyte nanoparticles through electrostatic interactions between the negatively charged OVA proteins and positively charged polyampholyte nanocarriers. Previously, we used PLL-DDSA (5)-SA (65) as an anionic nanocarrier for delivery; however, to incorporate anionic proteins onto the nanocarrier, it was necessary to tune the surface charge of nanocarriers toward cationic. As shown in **Figure S3A**, after being condensed with OVA proteins, the size of polyampholyte nanoparticles increased, demonstrating that adsorption of OVA proteins

had occurred. The average hydrodynamic size of PLL-DDSA(3)-SA(10) increased from 16.7 ± 0.3 to 30.1 ± 4.9 nm (**Figure S2A** and **S3A**). Conversely, the surface charge of ε-PLL markedly decreased from 26.5 ± 0.87 to 15.6 ± 3.33 mV. Similarly, polyampholyte nanoparticles also showed an equivalent trend, with the surface potential declining from 13.3 ± 4.19 to 4.40 ± 1.76 mV (**Figure S3B**).

Cytotoxicity of Polyampholytes. The in vitro toxicities of PLL alone and polyampholytes after modification with DDSA and SA were determined by MTT assay. **Figure S4** shows the cell viability of different polymers after treatment with different concentrations for 24 h. The cell viability was low in the case of PLL; it was approximately 60% at 1 mg/mL. At the same concentration, the polyampholyte nanocarrier exhibited a cell viability of nearly 69%. The lower cell viability of PLL may be due to positive surface charge as shown in **Figure S2B**. However, after formation of polyampholyte nanoparticles through slight modification of ε-PLL, the viability of the cells was increased owing to a decrease in the magnitude of the zeta potential (**Figure S2B)**.

Influence of Ice Crystallization-Induced Continuous Freezing on the Adsorption of Protein-Nanocarrier Complexes.

In the present investigation, NIH3T3 cells at a density of 1×10^4 cells/mL were loaded with FITC labeled-OVA incorporated with the polyampholyte nanoparticles PLL-DDSA (3)-SA(10) (2 mg protein and 1 w/w % nanoparticles in the cell suspension) in the presence of 10% DMSO as well as 10% PLL-SA cryoprotective solution. This mixture was placed into cryo-straws and plunged into a freeze controller programmed to gradually decrease the temperature at 1 °C/min. Following further temperature decrease, the samples were taken out from the freeze controller bath at specific temperatures and thawed at 37 °C, and the cell viability was assessed in the presence of cryoprotectant. We found that the use of 10% DMSO as well as 10% PLL-SA as cryoprotectants

both yielded living cells **(Figure S5**), with polyampholyte supporting a higher cell viability compared to DMSO (**Figure S5**). The unique cryoprotective ability with low toxicity of polyampholytes compared with DMSO is in agreement with our previous results.[16,17]

We also examined the adsorption of protein-nanocarrier complexes at different freezing temperatures. The CLSM images revealed that the adsorption of green FITC-labeled OVA proteins with PLL-DDSA (3)-SA (10) in the presence of DMSO as a cryoprotectant was markedly improved upon temperature decrease (**Figure 1A-F)**, and the performance progressively increased with continuously reduced temperatures. This outcome illustrates the role of sustained freezing as the influencing factor for protein adsorption. In comparison, when the polyampholyte cryoprotectant was used, the adsorption of OVA proteins was effectively enhanced, indicating that this cryoprotectant could afford better performance for the adsorption of protein-nanocarrier complexes (**Figure 1G-L).** Furthermore, quantification of fluorescence intensity from FITC-OVA proteins confirmed that polyampholyte cryoprotectant was more effective than DMSO (**Figure 1M**). The difference in adsorption of protein nanocarrier complexes by continuous freezing between the two cryoprotectants may be due to the difference in freeze concentration.

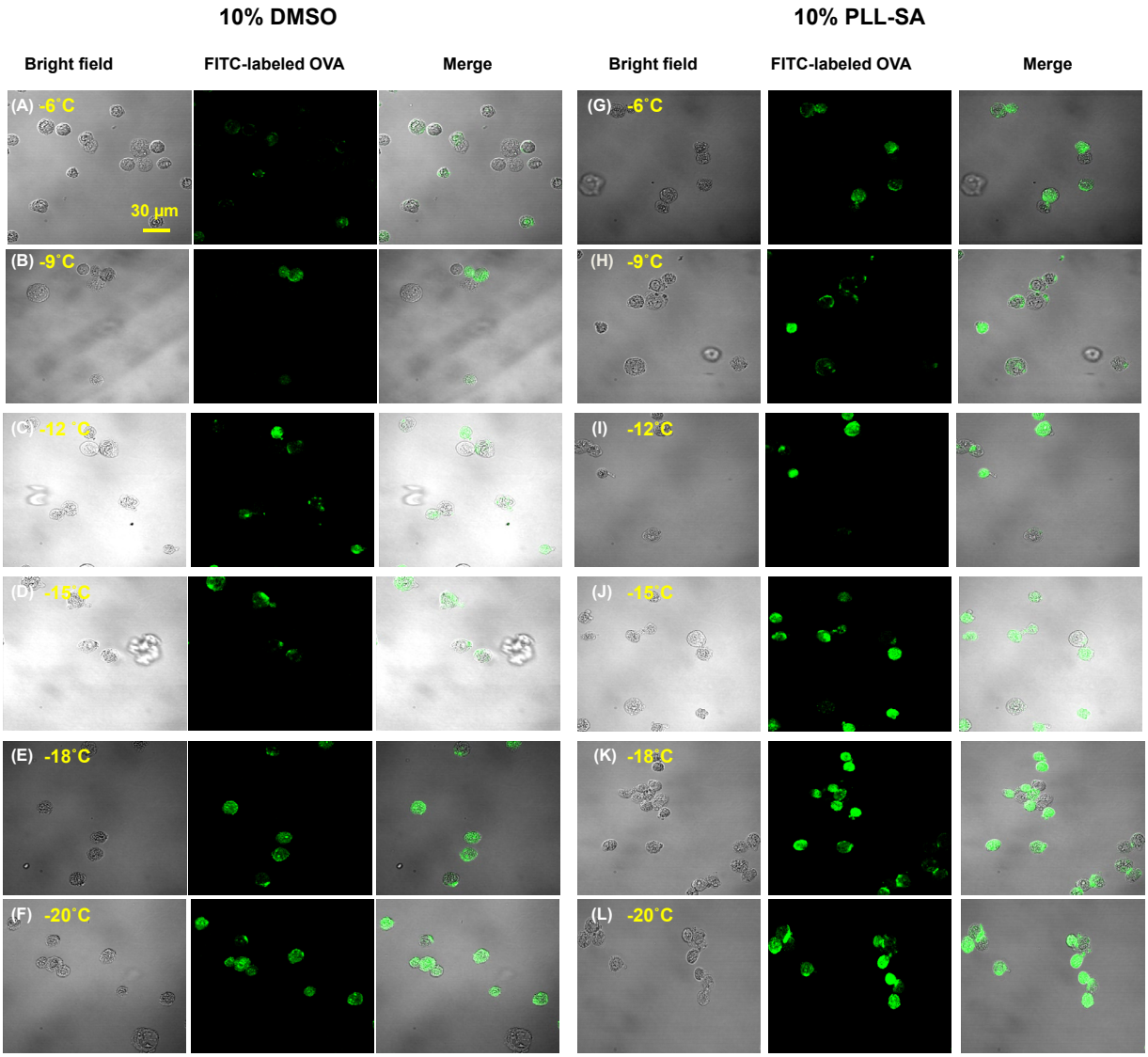
10% DMSO
10% PLL-SA
Bright field
FITC-labeled OVA
Merge
Bright field
FITC-labeled OVA
Merge
(A) -6˚C
30 μm
(B) -9˚C
(C) -12˚C
(D) -15˚C
(E) -18˚C
(F) -20˚C
(G) -6˚C
(H) -9˚C
(I) -12˚C
(J) -15˚C
(K) -18˚C
(L) -20˚C

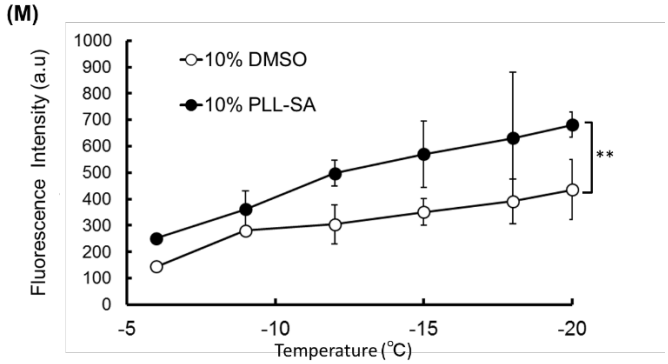
(M)
Fluorescence Intensity (a.u)
1000
900
800
700
600
500
400
300
200
100
0
10% DMSO
10% PLL-SA
**
-5
-10
-15
-20
Temperature (℃)

Figure 1 CLSM images for adsorption of FITC-labeled OVA protein loaded with PLL-DDSA(3)-SA(10) in the presence of cryoprotectants after being frozen at the rate of 1 °C/min for different temperatures with ice seeding (A-F), 10% DMSO (G-L), and 10% PLL-SA (M). Mean fluorescence intensity of adsorbed FITC-labeled OVA after freezing as determined by CLSM. Scale bar: 30 μm. Data are expressed as the mean ± SD. **p<0.01

Furthermore, we examined the stability of the protein-nanocarrier complex at low temperatures, and we determined the particle size change of the protein-nanocarrier complex (OVA-loaded PLL-DDSA (3)-SA (10)) in the presence of PLL-SA cryoprotectant dispersed in PBS(−) buffer (**Figure S6**). After being frozen at different temperatures and ice seeding, the solution was thawed and particle size was evaluated. We found the particle size did not change on exposure to different temperatures in the presence of cryoprotectant (**Figure S6**).

Freeze Concentration Factor of Cryoprotectants Alone or in Combination with Protein-Nanocarrier Complexes.

It is important to investigate the concentration ratio of the freeze-concentrated matrix in the unfrozen milieu. In one report, Miyawaki et al. proposed a generalized model to show the acceleration of freeze concentration in the form of a freeze concentration factor (α) during the frozen state.[18] Theoretically, the term (α) is related to the freezing point depression and was estimated from the analysis of the fraction of frozen water.

Specifically, the freeze concentration factor (α) is described as:

$$\alpha = \frac{[freezable\ water(Ffw)]}{[Unfrozen\ water\ (Ffw - Ff)]} \quad (4)$$

where Ff= the fraction of frozen water in the total water (g-frozen water/g-total water) and the fraction of freezable water (Ffw) can be determined by the equation:

$$Ffw = \frac{Xw - Xuf}{Xw} \quad (5)$$

where Xw = water content (g-water/g-total mass) and Xuf = unfreezable water content (g-water/g-total mass).

In Eq.(5), *Xuf* has been measured by using differential scanning calorimetry[30-32] and the fraction of frozen water in the freezable water (g-frozen water/g-freezable water) at a particular temperature T (°C) was described as:

$$\frac{Ff}{Ffw} = (1 - \frac{Tf}{T}) \quad (6)$$

where Tf = freezing point of the system (°C).

From the above equation, the unfrozen water fraction in the freezable water can be obtained as:

$$\frac{Ffw - Ff}{Ffw} = \frac{Tf}{T} \quad (7)$$

Combining equations 4 and 7, the temperature-dependent freeze-concentration factor is described by a simple equation with the only one parameter *Tf* as follows:

$$\alpha = \frac{T}{Tf} \quad (8)$$

The Tf value of 10% DMSO with and without the protein nanocarrier complex was found to be −3.725 and −4.475, respectively (**Figure 2A)**. In particular, 10% PLL-SA showed a very large difference (Tf= −0.683) when compared to 10% DMSO. However, when protein-nanocarrier complexes were added to 10% PLL-SA, a somewhat lower Tf (approximately −0.6) was obtained **(Figure 2 A).** The large difference between the Tf values reflects the distinction between the two

different cryomaterials. Notably, Tf of the protein-nanocarrier complex was −0.403 without incorporation of any cryoprotectants.

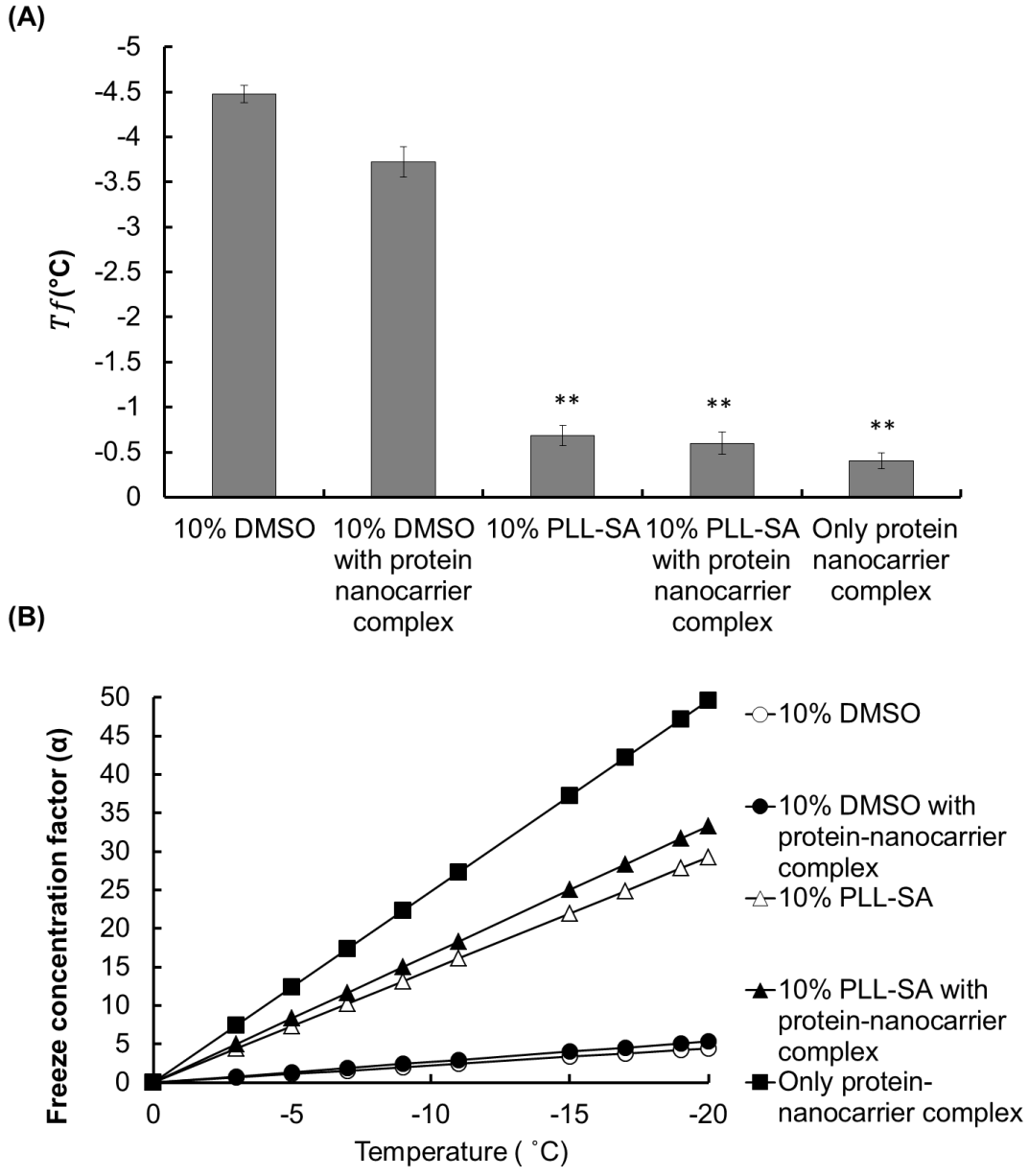

Figure 2. Estimation of freezing point (Tf) and freeze concentration factor (α) during freezing. (A) Determination of the freezing point of 10% DMSO without or with protein nanocarrier complex (OVA-loaded PLL-DDSA (3)-SA (10)), 10% PLL-SA without or with protein-nanocarrier complex, and protein-nanocarrier complex alone without cryoprotectant. (B) Based on the freezing point of the respective samples, freeze concentration factor (α) was calculated at

particular temperatures (0, −3, −5, −7, −9, −11, −15, −17, −19, and −20 °C). The graph shows the freeze concentration factor plotted against the specific temperature. Data are expressed as the mean ± SD, **p<0.01

This result signifies that when macromolecules such as polymers or proteins are present, the behavior of water during freezing is modified. Freezing point depression can be explained by the colligative properties. Although 10% DMSO exhibited a marked freezing point depression, 10% PLL-SA was found to exhibit a lower depression effect, possibly because of the low value of the molar mass of the molecules in the system resulting from the long chain-like structure of polyampholytes.

When a protein-nanocarrier complex is frozen, the complex is concentrated following ice crystal formation. Owing to this "change in concentration", the protein-nanocarrier level is elevated by a factor termed "α," which represents the freeze concentration factor in the freeze-induced concentration. Equation (8) shows the formula for the estimation of the "α" value. Accordingly, by using the freezing point (Tf) value, we calculated α values at different temperatures of interest. For example; Tf of 10% DMSO was found to be −4.475 as shown in **Figure 2 A**, and the temperature of interest (T) is −20 °C, yielding:

$$\alpha = \frac{-20}{(-4.475)} = 4.46$$

Therefore, by this method, the concentration factor of each sample can be easily calculated at different temperatures after determining the freezing point (Tf) value from **Figure 2A**. The graph plotted between the concentration factor and temperature using equation (8) is shown in **Figure 2B**. We estimated the freeze concentration factor of all samples including 10% DMSO, 10% DMSO with protein-nanocarrier complex, 10% PLL-SA, 10% PLL-SA with protein-nanocarrier

complex, and protein-nanocarrier complex without cryoprotectant. We found a large difference in the freeze concentration factor for DMSO and PLL-SA at the given temperatures (**Figure 2B**). For example, α was 33.33 using 10% PLL-SA in a system, whereas for 10% DMSO, α was restricted to 4.46. Based on this outcome, 10% PLL-SA was approximately 8-fold more concentrated compared with DMSO at −20 °C.

In Situ Fluorescence Microscopy Observation during Cell Freezing in the Presence of Protein-Nanocarrier Complex and Polyampholyte Cryoprotectant. In our prior examination, we found that the concentration factor notably increases during freezing for polyampholyte cryoprotectants incorporated with protein nanocarrier complexes. Therefore, to better understand the role of ice crystal-induced freeze concentration for the adsorption of protein-nanocarriers onto the cell membrane, we investigated the freezing process through fluorescence microscopy. The proteins were labeled with TR and the nanocarriers (PLL-DDSA(3)-SA(10)) were stained with FITC. To perform the experiment, 1×10^4 NIH3T3 cells/mL mixed with protein-nanocarrier complex (OVA-loaded PLL-DDSA(3)-SA (10)) in the presence of 10% PLL-SA were placed on a glass slide, covered, and loaded on a cooling stage programmer to cool the slide at 1 °C/min without a thawing procedure. Figure 3A-G shows the fluorescent images of cells laden with protein-nanocarrier complexes to compare between the normal condition and the freezing state. The fluorescence of OVA and PLL-DDSA (3)-SA (10) was very weak at 25 °C or even at −6, or −9 °C (Figure 3A-C). Notably, the fluorescence was drastically increased when the temperature reached −12 °C (Figure 3D). This is because at lower temperatures, the chances for the formation of ice crystals are greater, which leads to more rapid ejection of the protein-nanocarrier complexes, ultimately increasing the concentration (Figure 3D-G).

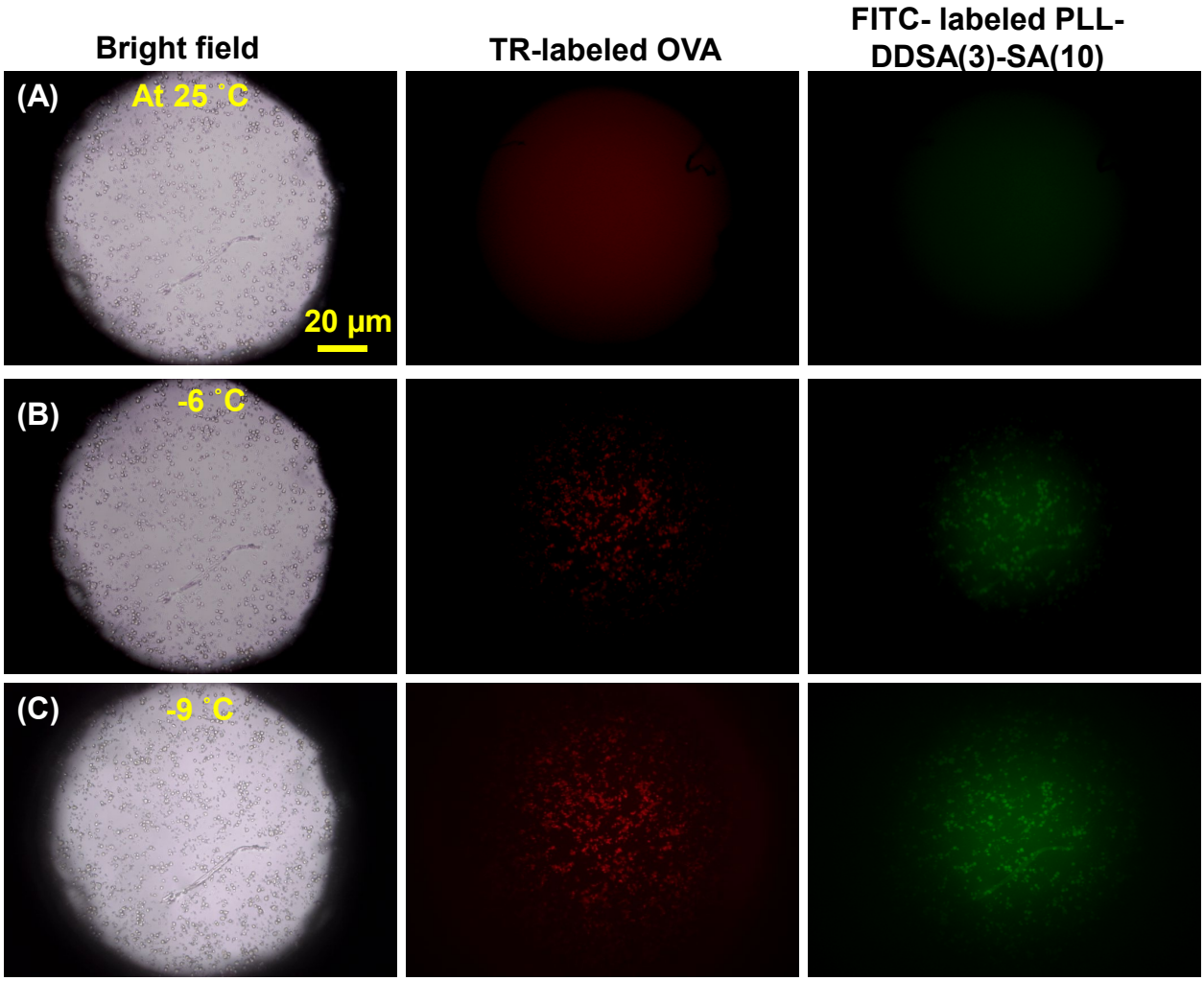
Bright field
TR-labeled OVA
FITC- labeled PLL-DDSA(3)-SA(10)
(A)
At 25 ˚C
20 μm
(B)
-6 ˚C
(C)
-9 ˚C

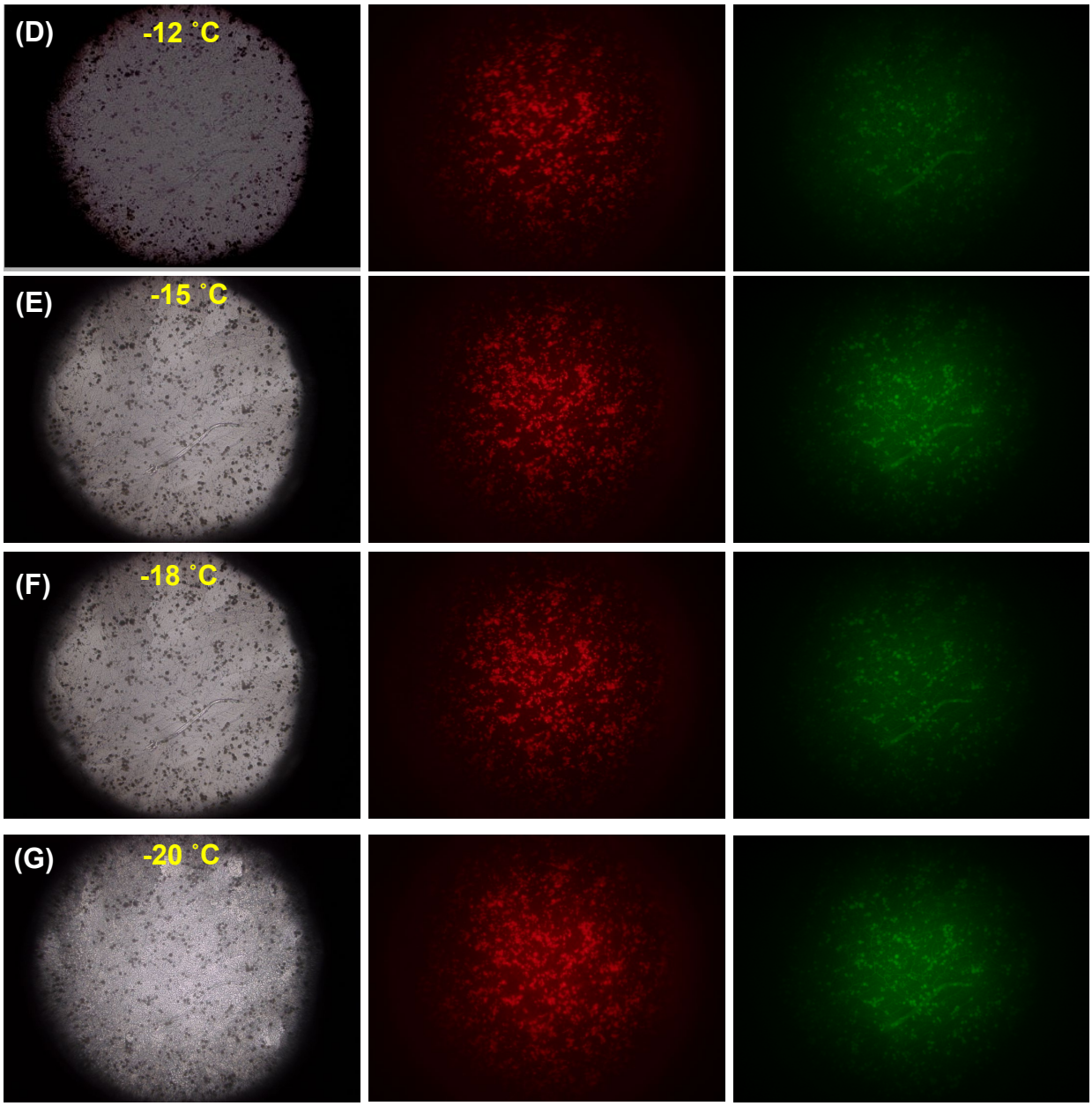

Figure 3. Fluorescence images of NIH3T3 cells loaded with the mixture of protein-nanocarrier complexes (OVA protein loaded with PLL-DDSA(3)-SA(10)) in the presence of 10% polyampholyte cryoprotectant during freezing. The PLL-DDSA(3)-SA(10)) complex was labeled with FITC and OVA protein was labeled with TR. The cell solution was placed on a glass slide loaded on a cooling stage using programmable freezing at the rate of 1 °C/min without thawing. Scale bar: 20 µm.

Internalization of OVA Proteins Loaded with PLL-DDSA(3)-SA(10) in the Presence of Cryoprotectants after the Thawing Procedure. We next sought to evaluate the internalization of the protein-nanocarrier complex through the course of freezing followed by thawing. The cells and protein-nanocarrier complex were subjected to the ice crystal-induced freezing and the samples were taken out at specific temperatures, thawed at 37 °C, seeded onto a glass bottom dish, and observed through CLSM. **Figure 4A, B** displays the merged images of TR-labeled OVA protein and FITC-labeled polyampholytes. Furthermore, when we attempted to observe the effect of cryoprotectants on the internalization of proteins, we found that 10% PLL-SA cryoprotectant exhibited enhanced internalization of protein-nanocarrier complexes compared with 10% DMSO ((**Figure 4A, B**). These results indicate that the large acceleration of protein-nanocarrier complex diffusion inside the cells in the case of 10% PLL-SA may be a consequence of the difference in freeze concentration as determined in our previous observation (**Figure 4B**).

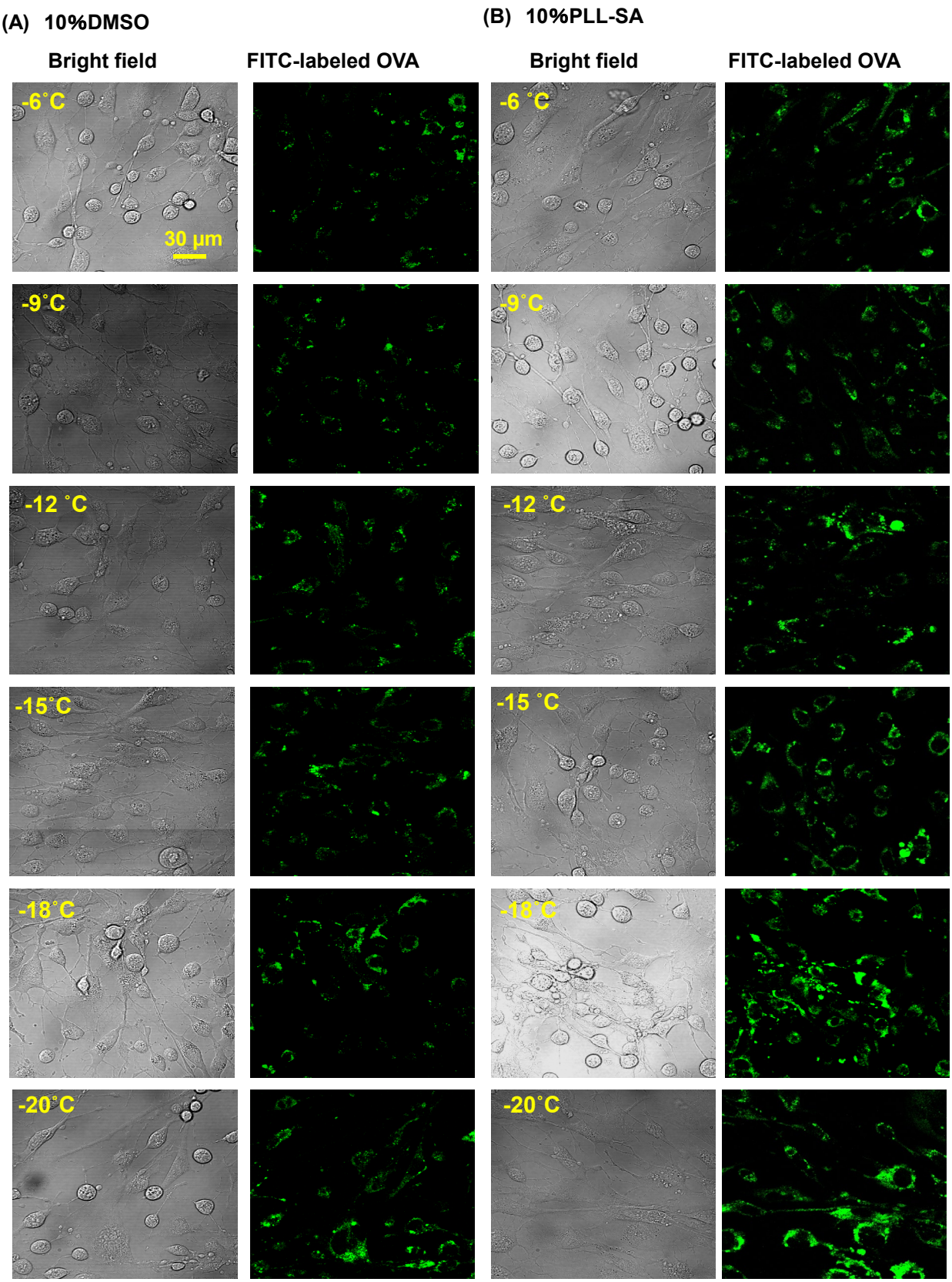
(A) 10%DMSO
(B) 10%PLL-SA
Bright field
FITC-labeled OVA
Bright field
FITC-labeled OVA
-6˚C
30 μm
-6 ˚C
-9˚C
-9˚C
-12 ˚C
-12 ˚C
-15˚C
-15 ˚C
-18˚C
-18˚C
-20˚C
-20˚C

Figure 4 CLSM analysis of NIH3T3 cells showing internalization of protein-nanocarrier complexes ((OVA protein loaded with PLL-DDSA(3)-SA(10)) after thawing. The OVA protein was labeled with TR, whereas PLL-DDSA(3)-SA(10) was labeled with FITC. (A) 10% DMSO (B) 10% PLL-SA. Scale bar: 30 μm

DISCUSSION

Protein-based therapeutics have widespread applications in biomedical engineering and regenerative medicine.[33] This study shows the use of an ice crystal-induced freeze concentration approach for cytoplasmic internalization of proteins into cells. However, before this method can be employed, it is very important to develop a carrier. Carrier use not only increases the efficacy of cytoplasmic protein delivery but also preserves the integrity of proteins by adsorption or encapsulation. Therefore, first we developed a polyampholyte-based nanocarrier for safe and highly efficient delivery into cells. The size of the polyampholyte is based on hydrophobic interactions resulting in the formation of self-assemblies. Previously, Shen et al. demonstrated the use of polyamino acids to form protein nanocarriers, prepared by grafting cationic amino acid (L-Arg) to γ-poly glutamic acid by inter/intra-molecular electrostatic interactions when the polymer was dispersed into water, in a manner comparable to nanogels.[34]

In our previous study, we reported the utilization of an ultra-cold freezing-induced strategy as a protein delivery system.[7,8] The protein-nanocarrier complex-loaded cells were exposed directly to −80 °C for 24 h. However, long-term exposure of proteins at ultra-cold temperatures can lead to poor stability, reducing their therapeutic activity and rendering them highly susceptible to loss caused by proteolysis, aggregation, unfolding, and denaturation.[35,36] Therefore, it is important to modulate the temperature conditions to protect the system from freezing damage. In the present

experiment, we thus optimized the freezing conditions using different temperatures followed by ice seeding. Ice seeding is a process that induces ice nucleation using cold tweezers. Previously, this process has been adapted for embryo cryopreservation, particularly for human oocytes and ovarian tissues, for which the process of ice seeding is essential as it enhances the dehydration of the cells by extracellular ice crystallization at the freezing rate of 0.20 °C/ min.[37] In practice, the cell viability is entirely dependent on the freezing rate. With slow freezing, embryos are at higher risk of excessive cell dehydration owing to prolonged exposure to high concentration of solutes, which negatively affects cell viability.[38] Conversely, a fast cooling rate is more likely to result in the formation of a large number of small-sized intracellular ice crystals. These are unable to maintain equilibrium and cause intracellular ice formation, which is lethal for cells and comprises a major cause of cell death during cryopreservation.[39] Therefore, the cooling rate must be carefully optimized to reduce the long-term exposure of cells to the frozen state but also to avoid the damaging effects of intracellular ice formation. Normally, a cooling rate of 1 °C/min is preferred for a wide variety of cells.

The utilization of cryoprotectants was extremely important in this study for cell survival. Cryoprotectants such as DMSO, which has been considered the most effective cryoprotective agent, are also used to protect cells from freezing damage and also to minimize the detrimental effects of increased solute concentration and ice crystal formation.[40] However, their toxicity[41] and ability to disrupt the differentiation of neuron-like cells, cardiac mycocytes, and granulocytes comprise major issues that further limit their use.[42–44] Hence, to remove these barriers, our group previously developed a new polyampholyte-based cryoprotectant to protect cells from freezing damage while maintaining high cell viability.[16] In particular, the unique polyampholyte-based cryoprotectant was found to retain the differentiation capabilities of rat and human mesenchymal

stem cells without serum proteins. The mechanism underlying the cryoprotection ability of polyampholytes is under investigation but this cryoprotectant has the unique property of efficiently preserving the cell membrane as reported in various studies.[45-50]

In addition, as most proteins are known to be susceptible to aggregation in freezing conditions, the use of cryoprotectants in protein delivery systems is very important. Therefore, it is necessary to ascertain the aggregation behavior of protein-nanocarrier complexes at low temperatures in the presence of the chosen cryoprotectant. **Figure S6** shows that the particle size did not change in relation to temperature. After thawing, the size was comparable between the initial temperature of −6 °C to the final temperature of −20 °C. These results indicate that OVA-loaded PLL-DDSA (3)-SA (10) nanoparticles are stable and do not change in size after exposure to low temperatures over a short time span.

Our next step was to determine the concentration involved during the freezing procedure. The concentration of protein-loaded delivery systems impacts the efficacy of cargo delivery to the cytoplasm at the target site. Freeze concentration can thus facilitate intracellular protein delivery. Generally, during spontaneous cooling from −5 to −45 °C, the solutes are excluded from the ice crystals, resulting in phase separation. Before freezing actually occurs, the solution is in thermodynamic equilibrium and the concentration of any solute is uniform in the unfrozen system. However, when freezing begins in the system, the growth of ice crystals separates the ions and salt of solutes and compresses the non-frozen region. In particular, in some chemical reactions, the rate acceleration in the frozen system is fully dependent on the concentration effect of aqueous solutions through ice crystal formation. For example, Miyawaki et al. demonstrated the use of a freeze concentration approach in apple juice to obtain high-quality concentrated sugar levels. The

obtained concentrate product was subsequently fermented to produce apple wine with an alcohol content higher than 10%.[51]

Miyawaki et al. presented a generalized equation to determine the freeze concentration involved during freezing.[31-32] As indicated in equation (8), the freeze concentration factor (α) is inversely proportional to the freezing point of the solution. Decreasing the freezing point reduces α because of the increase in the magnitude of the denominator. Therefore, the polyampholyte cryoprotectant has a higher freeze-concentration ratio because of the higher freezing point of the solution. We found in this study that the polyampholyte cryoprotectant had a high freeze concentration compared with DMSO **(Figure 2B)**. Notably, without cryoprotectant, the protein-nanocarrier complexes had very high α values as opposed to those with cryoprotectants in the same condition (**Figure 2B**). This may possibly be due to an increase in mobility and viscosity in the unfrozen milieu because of escalating strong intermolecular interactions during freezing.

Regardless, these results confirmed the findings of our prior investigation that the gradual decrease of freezing temperatures increases the freeze-concentration ratio of protein nanocarrier complexes with incorporated polyampholyte cryoprotectant. This combination leads to enhanced adsorption of protein-nanocarrier complexes across the periphery of the cell membrane (**Figure 1G-L**). These outcomes clearly suggest that freezing and cryoprotectant together play an important role in efficacy of the delivery system.

Furthermore, to observe the influence of ice crystal-induced freezing on adsorption of the protein nanocarrier complex, we investigated using a fluorescence microscope. We found that the considerable increase in concentration upon continuous temperature decrease could increase the interaction with the cell membrane, resulting in adsorption across the periphery of the membrane (Figure 3B-C). Moreover, the change in the morphology of the cells after the formation of ice

crystals around the cells was easily seen via bright field images (Figure 3D-G). Additionally, the adsorption of protein-nanocarrier complexes was higher at lower temperatures (Figure 3D-G). This result indicated the significance of freezing for the internalization of therapeutic agents within the cells. However, prolonged exposure of cells to low temperature affords the possibility of formation of intracellular ice crystals that may the damage cells. Therefore, the thawing process is extremely important after the freezing procedure for safe delivery of the therapeutic agent. Consequently, we observed the internalization of protein-nanocarrier complexes after thawing. We previously demonstrated that adsorption was fully dependent on the freezing process. The next step was therefore to examine the internalization behavior of protein-nanocarrier complexes. We found that proteins are subjected to more internalization in the presence of 10 % PLL-SA rather than with 10 % DMSO (**Figure 4A, B**). This is might be due to high the freeze-concentration ratio. In our investigation, we found that 10% PLL-SA had remarkably higher adsorption (**Figure 1 G-L**), and the same phenomenon was also observed for internalization. This is because the adsorption and internalization of proteins into the cells generally have a linear relationship, as the number of particles that adhere to the cell membrane will reflect that of particles being transferred inside the cells, as has been observed in our previous studies.[7, 8,52,53] Overall, this detailed study demonstrated the efficient use of the ice crystal-based freezing approach for internalization of proteins with the help of a unique polyampholyte cryoprotectant.

CONCLUSIONS

In this study, we used ice crystal-induced sustained freezing for intracellular protein delivery, which affords decreased process time and improved delivery safety, and obviates the requirement of extreme ultra-cold temperature. The main finding of our study is that increased freeze concentration shows a direct relationship with the adsorption and internalization of protein-nanocarrier complexes inside the cells. In addition, considerable attention was paid to the influence of cryoprotectants in the delivery system. Our findings particularly suggest that polyampholyte cryoprotectants exhibit a high freeze concentration compared with DMSO because of less freezing point depression of the latter during freezing. When cells were treated with protein-nanocarrier complexes followed by polyampholyte cryoprotectant and ice crystal-induced freezing, the protein cargos were effectively adsorbed and simultaneously internalized into the cytoplasm because of the high freeze concentration. Taken together, these data illustrate a unique freezing strategy that was able to deliver proteins efficiently into the cytosol of cells, afford stability in the presence of polyampholytes as a cryoprotectant, and circumvent the exposure to ultra-cold temperature for extended periods. In our future studies, we plan to assess the utility of the ice-crystallization-induced freeze concentration method for cancer therapy as well as other therapeutic applications.

ASSOCIATED CONTENT

Supporting information. The following files are available free of charge.

Scheme S1; Files S1-S6 (file type, i.e., PDF)

AUTHOR INFORMATION

Corresponding Author

*E-mail: mkazuaki@jaist.ac.jp. Tel: +81-761-51-1680; Fax: +81-761-51-1149

Author Contributions

The manuscript was written through contributions of all authors. All authors have given approval to the final version of the manuscript.

ACKNOWLEDGMENT

This study was supported in part by a Grant-in-Aid, KAKENHI (16K12895), for scientific research from Japan Society for the Promotion of Science and a Collaborative Research Project organized by the Interuniversity Bio-Backup Project (IBBP).

ABBREVIATIONS

CLSM, confocal laser scanning microscopy; CS, calf serum; DDSA, dodecenylsuccinic anhydride; DMEM, Dulbecco's modified Eagle's medium; DMSO, dimethyl sulfoxide; FITC, fluorescein isothiocyanate; MTT, 3-(4,5-dimethyl thial-2yl)-2,5-diphenyltetrazalium bromide; NMR, nuclear magnetic resonance; OVA, ovalbumin; PBS, phosphate buffered saline; PLL, ε-poly-L-lysine; SA, succinic anhydride, TR, Texas red sulfonyl chloride.

REFERENCES

(1) Li, J.; Zhang, L.; Liu, Y.; Wen, J.; Wu, D.; Xu, D.; Segura, T.; Jin, J.; Lu, Y.; Wang, H. An intracellular protein delivery platform based on glutathione-responsive protein nanocapsules. *Chem. Commun.* **2016**, *52*, 13608-13611.

(2) Dinca, A.; Chien, W.M.; Chin, M.T. Intracellular delivery of proteins with cell-penetrating peptides for therapeutic uses in human diseases. *Int. J Mol Sci.* **2016**, *17*(2), 263.

(3) Gehl, J. Electroporation: theory and methods, perspectives for drug delivery, gene therapy and research. *Acta Physiol Scand.* **2003**, *177* (4), 437-447.

(4) Huang, S.L. Liposomes in ultrasonic drug and gene delivery. *Adv. Drug Deliv. Rev.* **2008**, *60*, 1167-1176.

(5) Zhang, Y.; Yu, L.C. Single-cell microinjection technology in cell biology. *Bioessays.* **2008**, *30*, 606-610.

(6) Frey, W.; White, J.A.; Price, R.O.; Blackmore, P.F.; Joshi, R.P.; Nuccitelli, R.; Beebe, S.J.; Schoenbach, K.H.; Kolb, J.F. Plasma membrane voltage changes during nanosecond pulsed electric field exposure. *Biophys J.* **2006**, *90* (10), 3608-3615.

(7) Ahmed, S.; Hayashi, F.; Nagashima, T.; Matsumura, K. Protein cytoplasmic delivery using polyampholyte nanoparticles and freeze concentration. *Biomaterials*, **2014**, *35*, 6508-6518.

(8) Ahmed, S.; Fujita, S.; Matsumura, K. Enhanced protein internalization and efficient endosomal escape using polyampholyte-modified liposomes and freeze concentration. *Nanoscale*, **2016**, *8*, 15888-15901.

(9) Pham, Q.T. Advances in food freezing/thawing/freeze concentration and techniques. *Jpn J Food Eng*. **2008**, *9*, 21-32.

(10) Takemoto, H.; Miyata, K.; Ishii, T.; Hattori, S.; Osawa, S.; Nishiyama, N.; Kataoka, K. Accelarated polymer-polymer click conjugation by freeze-thaw treatment, *Bioconjugate Chem*., **2012**, *23*(8), 1503-1506.

(11) Takenaka, N.; Ueda, A.; Maeda, Y. Acceleration of the rate of nitrile oxidation by freezing in aqueous solution. *Nature* **1992**, *358*, 736-738.

(12) Bhatnagar, B.S.; Nehm, S.J.; Pikal, M.J.; Bogne, R.H. Post-thaw aging activity of lactate dehydrogenase. *J. Pharm, Sci*. **2005**, *94*, 1382-1388.

(13) Connolly, B.D.; Patapoff, T.W.; Cromwell, M.E.; Moore, J.M.; Lam, P. Protein aggregation in frozen trehalose formulations: Effects of composition, cooling rate, and storage temperature. *J. Pharm. Sci*. **2015**, *104*, 4170-4184.

(14) Jain, N. K.; Roy, I., Effect of trehalose on protein structure, *Protein Sci.*, **2009**, *18*(1), 24–36.

(15) Fonte, P.; Sousa, S.; Costa, A.; Seabra, V.; Reis S.; Sarmento, B. *Biomacromolecules*, **2014**, *15*(10), 3753–3765.

(16) Matsumura, K.; Hyon, S.H. Polyampholytes as low toxic efficient cryoprotective agents with antifreeze protein properties. *Biomaterials* **2009**, *30*, 4842-4849.

(17) Matsumura, K.; Kawamoto, K.; Takeuchi, M.; Yoshimura, S.; Tanaka, D.; Hyon, S.H. Cryopreservation of a two-dimensional monolayer using a slow vitrification method with polyampholyte to inhibit ice crystal formation. *ACS Biomater. Sci. Eng.*, **2016**, *2*(6), 1023-1029.

(18) Miyawaki, O.; Nishino, H. Kinetic analysis of freeze denaturation of soy protein by a generalized theoretical model for freeze-acceleration reaction. *J Food Eng.* **2016**,*190*, 109-115.

(19) Liu, L.; Fujii, T.; Hayakawa, K.; Miyawaki, O. Prevention of initial super cooling in progressive freeze concentration. *Biosci. Biotechnol. Biochem*. **1998**, *62*, 2467-2469.

(20) Yuba E.; Harada, A.; Sakanishi, Y.; Watarai, S.; Kono, K., A liposome-based antigen delivery system using pH-sensitive fusogenic polymers for cancer immunotherapy, *Biomaterials* **2013**, *34*(12), 3042-3052.

(21) De Jong, W.H.; Borm, P.J.A. Drug delivery and nanoparticles: Applications and hazards. *Int. J. Nanomedicine* **2008**, *3*(2), 133-149.

(22) Sakaguchi, N.; Kojima, C.; Harada, A.; Kono, K. Preparation of pH-sensitive poly(glycidol) derivatives with varying hydrophobicity: their ability to sensitize stable liposomes to pH. *Bioconjug Chem*, **2008**, *19*, 1040-1048.

(23) Lundy, B.B.; Convertine, A.; Miteva, M.; Stayton, P.S. Neutral polymeric micelles for RNA delivery. *Bioconjug Chem*, **2013**, *24*, 398-407.

(24) Li, Y.; Xiao, K.; Luo, J.; Lee, J.; Pan, S.; Lam, K.S. A novel size-tunable nanocarrier system for targeted anticancer drug delivery. *J Control Release*, **2010**, *144*, 314-323.

(25) Pisal, D.S.; Kosloski, M.P.; Balu-Iyer, S. V. Delivery of therapeutic proteins. *Pharm. Sci*., **2010**, *99*(6), 2557–2575.

(26) Soenen, S. J.; Parak, W. J.; Rejman, J.; Manshian, B. (Intra) cellular stability of inorganic nanoparticles" effect on cytotoxicity, particle functionality, and biomedical applications. *Chem. Rev*., **2015**, *11*, 2109–2135

(27) Fu, H.; Ding, J.; Flutter, B.; Gao, B., Investigation of endogenous antigen processing by delivery of an intact protein into cells. *J Immunol Methods* **2008**, *335*, 90-97.

(28) Yoshizaki, Y.; Yuba, E.; Komatsu,, T.; Udaka, K.; Harada, A.; Kono, K. Improvement of peptide-based tumor immunotherapy using pH-sensitive fusogenic polymer-modified liposome. *Molecules* **2016**, *21*, 1284.

(29) Song, C.; Noh, Y.W.; Lim, Y.T. Polymer nanoparticles for cross-presentation of exogenous antigens and enhanced cytotoxic T-lymphocyte immune response. *Int. J. Nanomedicine* **2016**, *11*, 3753-3764.

(30) Pham, Q.T., Willix, J. Thermal conductivity of fresh lamb meat, offal and fat in the range -40 to þ30 C: measurements and correlations. *J. Food Sci.* **1989**, *54*, 508-515.

(31) Pongsawatmanit, R., Miyawaki, O. Measurement of temperature-dependent ice fraction in frozen foods. *Biosci. Biotechnol. Biochem.* **1993**, *57*, 1650-1654.

(32) Pradipasena, P., Tattiakul, J., Nakamura, K., Miyawaki, O. Temperature dependence of fraction of frozen water in solutions of glucose and its oligomers, dextrans, and potato starch. *Food Sci. Technol. Res*. **2007**, *13*, 286-290.

(33) Mao, A.S.; Mooney, D.J. Regenerative medicine: Current therapies and future directions, *Proc. Natl. Acad. Sci*.**2015**, *112*, 14452-14459.

(34) Shen, H.; Akagi, T.; Akashi, M. Polyampholyte nanoparticles prepared by self complexation of cationized poly (*γ-glutamic acid) for protein carriers. Macromol. Biosci.* **2012***, 12,* 1100-1105.

(35) Smith, M. H.; Lyon, L. A. Tunable Encapsulation of Proteins within Charged Microgels, *Macromolecules*, **2011**, *44*, 8154-8160.

(36) Li,J. K.; Wang, N.; Wu, X. S. A novel biodegradable system based on gelatine nanoparticles and poly(lactic-co-glycolic acid) microsphere for proteins and peptide drug delivery. *Int. J. Pharm. Sci.*, **1997**, *86*, 891– 895.

(37) Zhang, J.M.; Sheng, Y.; Cao, Y.Z.; Wang, H.Y.; Chen, Z.J. Effects of cooling rates and ice-seeding temperatures on the cryopreservation of whole ovaries. *J Assist Reprod Genet*, **2011**, *28*, 627-633.

(38) Trad, F.S.; Toner, M.; Biggers, J.D. Effect of cryoprotectants and ice-seeding temperature on intracellular freezing and survivial of human oocytes. *Hum. Reprod.* **1999**, *14*, 1569-1577.

(39) Seki, S.; Mazur, P. The dominance of warming rate over cooling rate in the survival of mouse oocytes subjected to a vitrification procedure. *Cryobiology*, **2009**, *59*(1), 75-82.

(40) Baust, J.G.; Gao, D.; Baust, J.M. Cryopreservation: An emerging paradigm change. *Organogenesis* **2009**, *5*(3), 90-96.

(41) Fahy GM. The relevance of cryoprotectant ‘‘toxicity’’ to cryobiology. *Cryobiology* **1986**, *23*(1):1–13

(42) Oh, J.E.; Karlmark Raja, K.; Shin, J.H.; Pollak, A.; Hengstschlager, M.; Lubec, G. Cytoskeleton changes following differentiation of N1E-115 neuroblastoma cell line. *Amino Acids* **2006**, *31*, 289–298.

(43) Young, D.A.; Gavrilov, S.; Pennington, C.J.; Nuttall, R.K.; Edwards, D.R.; Kitsis, R.N. Expression of metalloproteinases and inhibitors in the differentiation of P19CL6 cells into cardiac myocytes. *Biochem Biophys Res Commun* **2004**, *322*, 759–765.

(44) Jiang, G.; Bi, K.; Tang, T.; Wang, J.; Zhang, Y.; Zhang, W. Down-regulation of TRRAP-dependent hTERT and TRRAP-independent CAD activation by Myc/Max contributes to the differentiation of HL60 cells after exposure to DMSO. *Int Immunopharmacol* **2006**, *6*(7), 1204–1213.

(45) Matsumura, K.; Bae, J.Y.; Hyon, S.H. Polyampholytes as cryoprotective agents for mammalian cell cryopreservation. *Cell transplantation* **2010**, *19*, 691-699.

(46) Matsumura, K.; Bae, J.Y.; Kim, H.H.; Hyon, S.H. Effective vitrification of human induced pluripotent stem cells using carboxylated ε-poly-L-lysine. *Cryobiology* **2011**, *63*(2), 76-83.

(47) Matsumura, K.; Hayashi, F.; Nagashima, T.; Hyon, S.H. Long-term cryopreservation of human mesenchymal stem cells using carboxylated poly-L-lysines

without the addition of proteins or dimethyl sulfoxide. *J Biomater Sci Polym Ed* **2013**, *24*, 1484-1497.

(48) Rajan, R.; Hayashi, F.; Nagashima,T.; Matsumura, K. Toward a molecular understanding of the mechanism of cryopreservation by polyampholytes: Cell membrane interaction and hydrophobicity. *Biomacromolecules* **2016**, *17* (5), 1882-1893.

(49) Vorontsov, DA.; Sazaki, G.; Hyon, SH.; Matsumura, K.; Furukawa, Y. Antifreeze Effect of Carboxylated ε-Poly-l-lysine on the Growth Kinetics of Ice Crystals. *J Phys. Chem. B.* **2014**,118,10240-10249.

(50) Mitchell, DE.; Cameron, NR.; Gibson, M. Rational, yet simple, design and synthesis of an antifreeze-protein inspired polymer for cellular cryopreservation. *Chem. Commnu.* **2015**,51,12977-12980.

(51) Miyawaki, O.; Gunathilake, M.; Omote, C.; Koyonagi, T.; sasaki, T., Take, H.; Matsumda, A.; Ishisaki, K.; Miwa, S.; Kitano, S. Progressive freeze-concentration of apple juices and its application to produce a new type apple wine. *J Food Eng.* **2016**,*171*,153-158.

(52) Ahmed, S.; Fujita, S.; Matsumura, K. A freeze concentration and polyampholyte-modified liposome-based antigen delivery system for effective immunotherapy. *Adv. Healthc Mater* **2017**, Doi 10.1002/adhm.201700207

(53) Ahmed, S.; Tadashi, N.K.; Watanabe, T.; Hohsaka, T. Matsumura, K.; Freezing-assisted gene delivery combined with polyampholyte nanocarriers. *ACS Biomater. Sci. E*ng. **2017**, *3*(8), 1677-1689.

ToC Figure

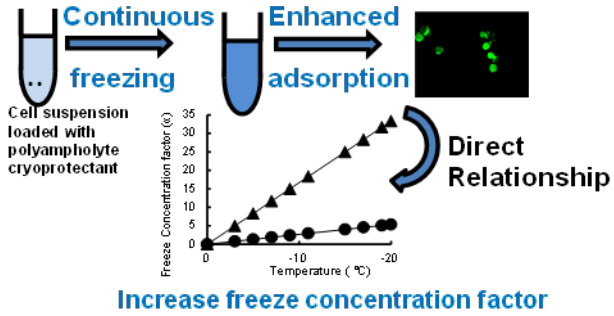
Continuous
freezing
Enhanced
adsorption
Cell suspension
loaded with
polyampholyte
cryoprotectant
Freeze Concentration factor (c)
35
30
25
20
15
10
5
0
0
-10
-20
Temperature (°C)
Direct
Relationship
Increase freeze concentration factor

Enhanced Adsorption of a Protein-Nanocarrier Complex onto Cell Membranes through High Freeze Concentration by a Polyampholyte Cryoprotectant

Sana Ahmed,[†] *Osato Miyawaki,*[‡] *and Kazuaki Matsumura**[,†]

[†]School of Materials Science, Japan Advanced Institute of Science and Technology, Nomi, Ishikawa 923-1292, Japan

[‡]Department of Food Science and technology, Tokyo University of Marine Science and Technology, 4-5-7 Konan, Minato-ku, Tokyo, 108-8477, Japan

Corresponding Author

*E-mail: mkazuaki@jaist.ac.jp. Tel: +81-761-51-1680; Fax: +81-761-51-1149

Table of contents:

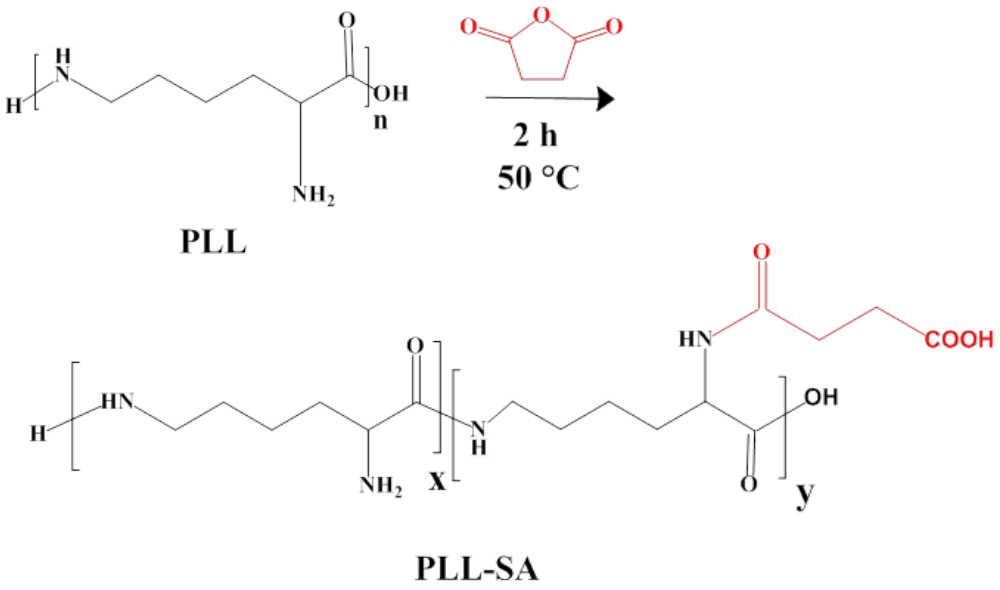

Scheme S1. Synthetic scheme for cryoprotective polyampholytes (PLL-SA).

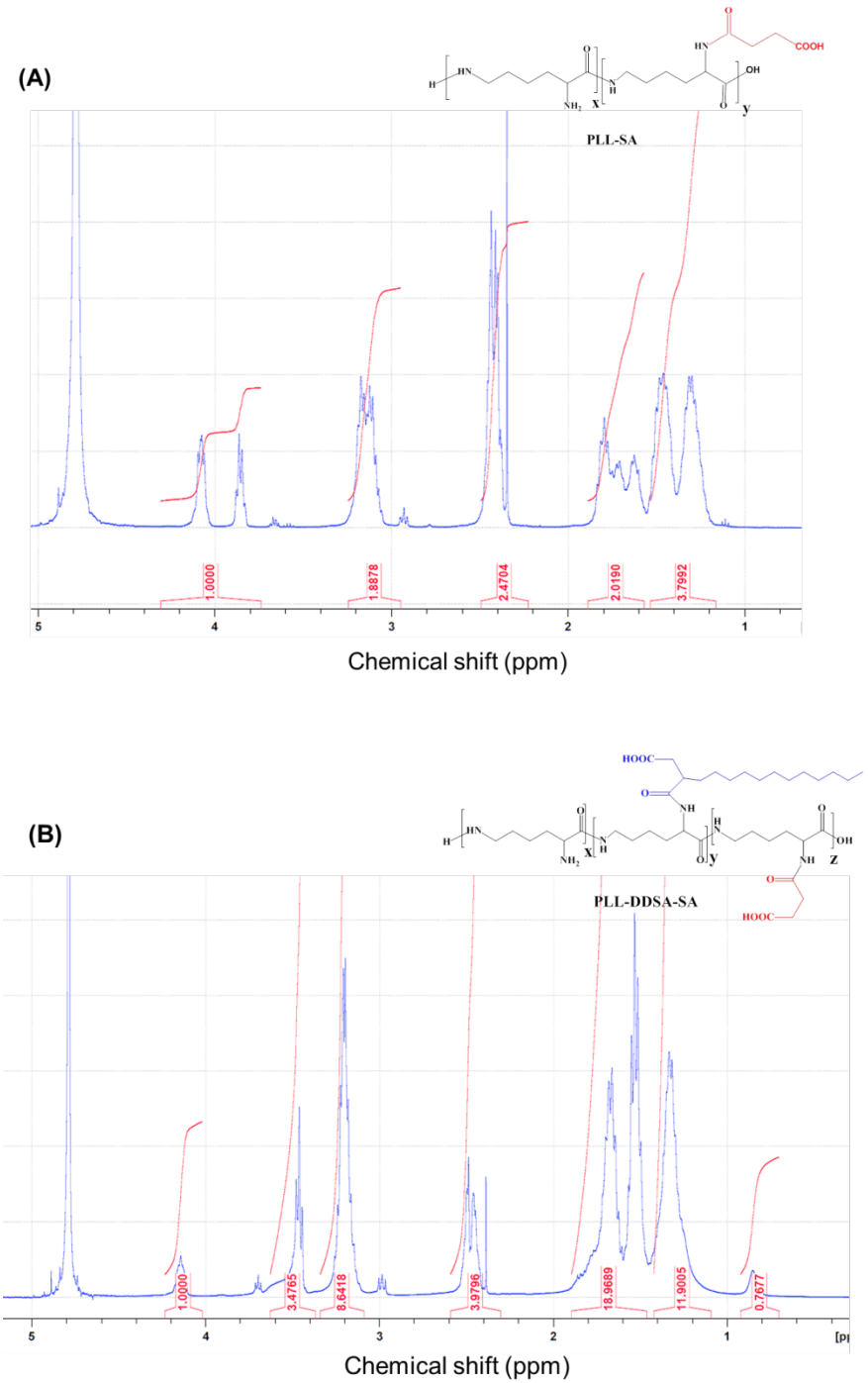

Figure S1. (A) ^{1}H NMR of PLL-SA (B) ^{1}H NMR of PLL-DDSA-SA

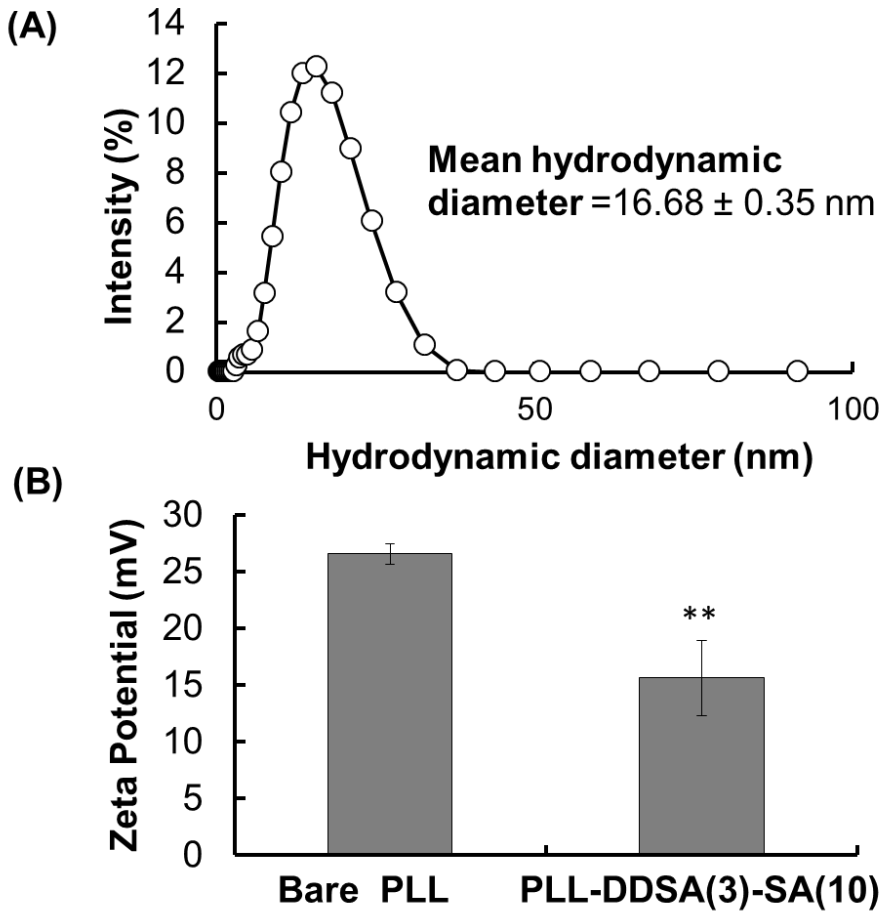

Figure S2. Characterization of bare PLL and hydrophobic polyampholyte (PLL-DDSA(3)-SA(10)) in PBS(−) buffer by using dynamic light scattering analysis. (A) Hydrodynamic diameter. (B) Zeta potential. Data are expressed as the mean ± SD. **$p<0.01$

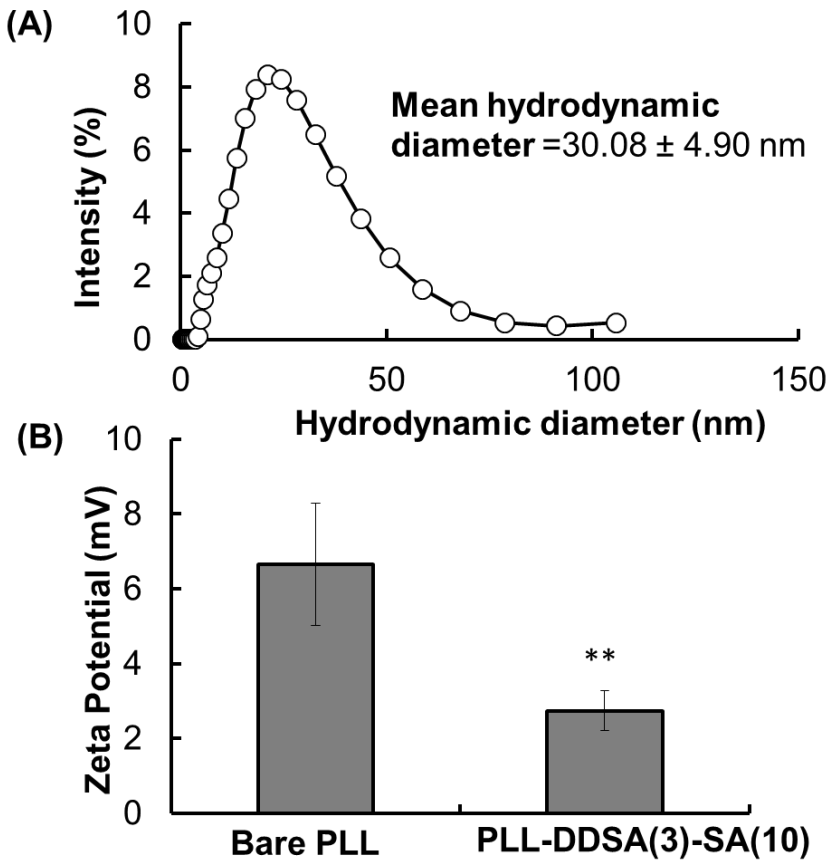

Figure S3. Characterization of OVA protein-loaded PLL or PLL-DDSA(3)-SA(10)) in PBS(−) buffer by using dynamic light scattering analysis. (A) Hydrodynamic diameter. (B) Zeta potential. Data are expressed as the mean ± SD. **p<0.01

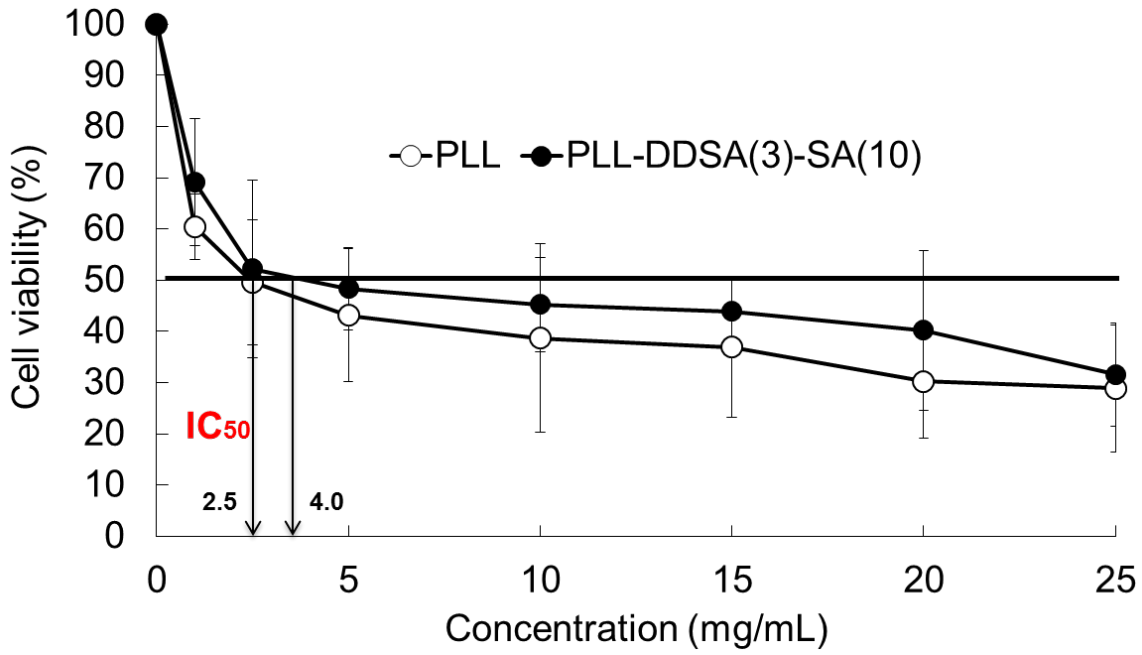

Figure S4. Cytotoxicity of bare PLL and hydrophobic polyampholytes (PLL-DDSA(3)-SA(10)). NIH3T3 cells were incubated with different concentrations of polymers, followed by MTT analysis. IC_{50} represents the concentration of nanoparticles that caused a 50% reduction in MTT uptake in a treated cell culture compared with an untreated cell culture. Data are expressed as the mean ± SD

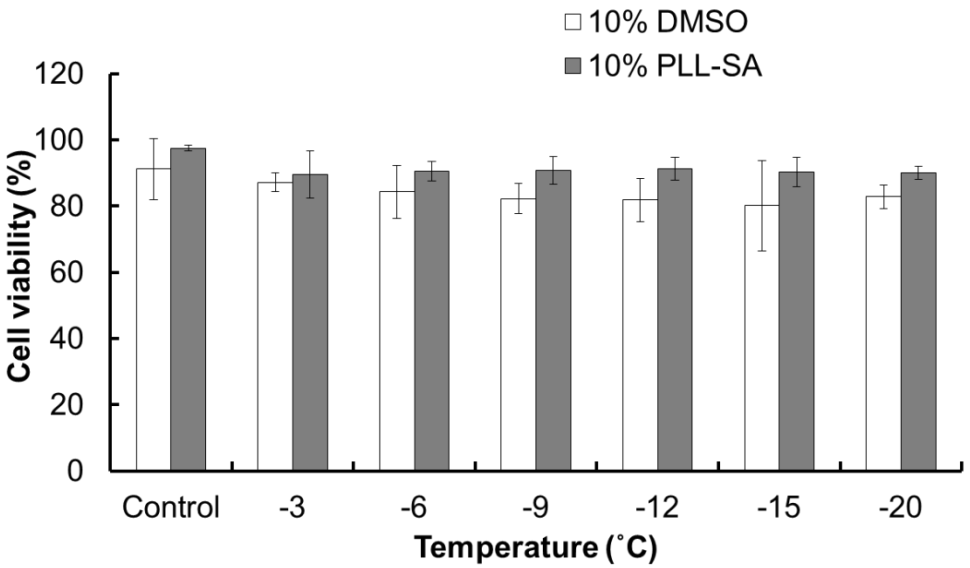

Figure S5. Cell viability on treatment with protein-nanocarrier complex (OVA protein loaded with PLL-DDSA(3)-SA(10)) at different temperatures (−3, −6, −9, −12, −15, and −20 °C) in the presence of 10% DMSO and 10% PLL-SA cryoprotectants frozen at the rate of 1 °C/min. Data are expressed as the mean ± SD

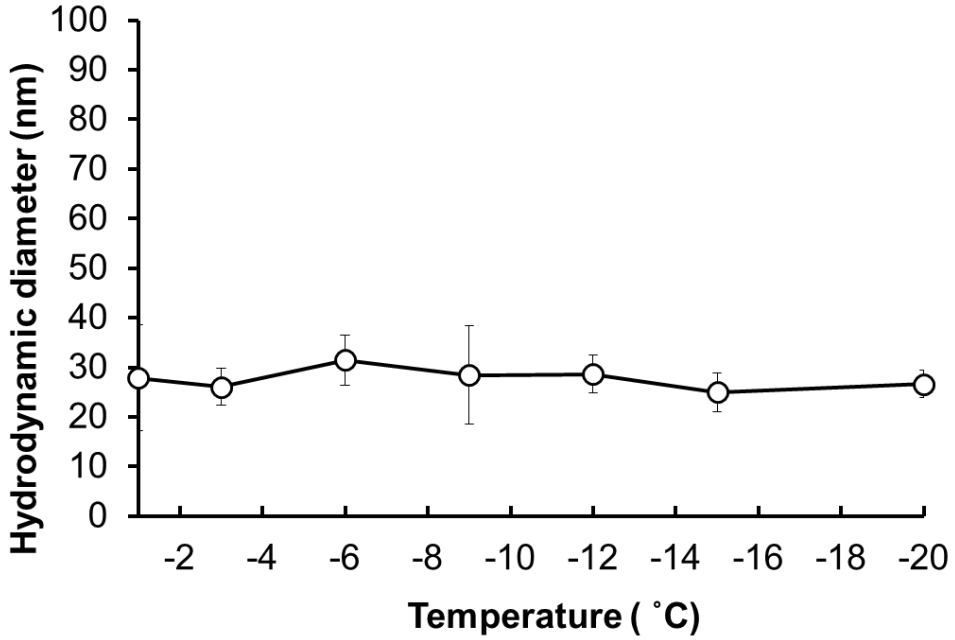

Figure S6. Change in hydrodynamic diameter of protein-nanocarrier complex (OVA-loaded PLL-DDSA (3)-SA(10)) with respect to temperature as determined by dynamic light scattering. Data are expressed as the mean ± SD